

A MODEL OF DEFORMATION GEOMETRY IN PIPE BENDING PROCESSES

Z. Ś L O D E R B A C H

OBR – GRE WROCŁAW

ul. Nyska 64, Wrocław, Poland

The paper presents a complete set of geometric relationships for logarithmic measures of longitudinal, circumferential and radial strains arising in bending of thin- and thick-walled pipes. The strain can be determined at each plane parallel to the principal plane of bending and at each plane perpendicular to them, so that each point of the bending zone is accounted for. The relationships have a direct reference to engineering practice since they express strains as functions of pipe geometry and bending process variables. The calculation results were compared with experimental data for the bend angle equal to 180° and the bending zone range index equal to 1 and 3. Suitable plots are incorporated.

NOTATIONS

R	bending radius, equal to the radius of the neutral surface;
R_0	radius of the neutral surface following bending;
y_0	displacement of the neutral surface with respect to the initial position;
d_{out}	outside diameter of a bent pipe (OD – engineering notation);
r_{out}	outside radius of a bent pipe;
d_{in}	inside diameter of a bent pipe (ID – engineering notation);
r_{in}	inside radius of a bent pipe;
g_0	initial thickness of a bent pipe;
R_i	larger running radius of a bend associated with longitudinal strain;
r_i	smaller running radius of a bend;
g_i	running thickness of a bend within the bending zone; ($i = 1$ for elongated fibres, $i = 2$ for compressed fibres);
α_g	bending angle measured over the bending zone, $\alpha_g \in [0^\circ; 180^\circ]$;
k	coefficient of the bending zone range as determined in actual tests. In theory, $k \in [1; \infty]$, but in practice $k \in [1; 10]$ should be sufficient. The coefficient may be also meant to determine the ratio of $\alpha_{g\text{max}} = 180^\circ$ to the actual value of α_g ;
α_0	bend angle (the angle by which a former or die is rotated); in theory, $\alpha_0 \in [0^\circ; \infty)$. Obviously, within the bending zone the two angles are equal ($\alpha_0 = \alpha_g$);
α	running angle of the bending zone determined at the principal bending plane and at planes parallel to it, $\alpha \in \left[0^\circ; \frac{\alpha_g}{2}\right]$;

β	running angle determined at planes perpendicular to the bending plane, $\beta \in [0^\circ; 90^\circ]$;
ξ	angle defining the bending zone at the principal plane of bending and at planes parallel to it, $\xi \in [0^\circ; \alpha_0]$;
θ	angle defining the cross-section contour of a bend as a closed path, $\theta \in [0^\circ; 360^\circ]$;
φ_1	logarithmic longitudinal strain at the bending plane;
φ_2	logarithmic circumferential strain at the plane perpendicular to the bending plane;
φ_3	logarithmic radial strain along the thickness;
φ_i	strain intensity, equivalent strain;
g_{\min}	minimum wall thickness at the elongated area;
g_{\max}	maximum wall thickness at the compressed area;
s	wall thickness index for a pipe, $s = \frac{g_0}{d_{\text{out}}}$, $s < 0.2$ – thin-walled pipe, $s > 0.2$ – thick-walled pipe, after [1];
e	ovality index of the cross-section, after [1];
A_1	ovality index of the cross-section, after [4];
d_1	outside pipe diameter as measured on finishing the bending process;
z_1, z_2	vertical and horizontal measure, respectively, associated with radius R_i .

1. INTRODUCTION

Piping stress and strain analysis is a complex and highly involved subject. This paper is concerned with only one fundamental problem – the determination of deformational characteristics of pipe bends fabricated from initially straight tube sections. The bends are regarded to be critical components of piping systems and their structural analysis is of utmost importance in the design.

The paper is aimed at deriving basic relationships for geometrical measures of deformation in bending of both thin- and thick-walled pipes. As it is generally known, the wall in a bent pipe gets thinner in the elongated fibre area and thicker in the area of compressed fibres. As a result, the initially circular cross-section assumes an oval form. Additionally, the overall shape of a pipe length is disturbed by buckling effects. The paper will be focussed on the ovalization effect due to the fact that wall thinning is not fully compensated by wall thickening at the other end of the diameter. The inescapable phenomena of wall thinning/thickening and warping as well as cross-section ovalization should be always under strict control [1].

The paper presents geometrical relationships for logarithmic measures of longitudinal, circumferential and radial strains. The measures may be determined at all planes parallel to the principal plane of bending and also at each plane perpendicular to them, i.e. throughout the whole bending zone. The assumed model accounts for material properties through one parameter defining the bending zone range. An additional assumption holds that the pipe material behaves like an incompressible continuous medium. Despite these limitations, the results yielded by the model are in very good agreement with experimental data presented in

[2], especially for elongated fibres. The relationships for logarithmic components of permanent strains involve the following arguments: bending radius and angle, geometrical characteristics of a pipe, angular coordinates α, β – used as parameters in defining the bending zone, and index k – for specifying the bending zone range.

Premature failure of pipe bends encountered in engineering practice are usually attributed to inadequate methods of structural analysis being currently in use in the design of pipelines [3 – 6]. A specific weakness of the available designer's knowledge is the lack of a precise method for determining an allowable wall thickness distribution at the apex of the maximum strain zone. With prior knowledge of strain and stress intensity components within the whole bending zone and especially at its apex portion, the pertinent stress analysis becomes much more reliable and so is the bend manufacture.

The bending zone is usually composed of two portions: bending zone (varying strain zone) and plateau zone (constant maximum strain zone). The first portion is found at the ends of a bend and its extent is affected by: the particular bending technique used, bending radius, type of material, pipe geometry. The available experimental evidence shows that more protruding and "sharp" mandrels together with smaller radii of bending and less ductile materials act all to decrease the bending zone extent and *vice versa*. The extreme cases involve either almost negligible bending zones or their expansion to cover the whole bend (with no plateau portion in between) [1].

There is enough of forensic analysis evidence to state that the onset of damage processes usually takes place near the middle of the elongated bend side. Initial microcracks grow fairly fast and since there are no crack arrest mechanisms, catastrophic leakage becomes imminent [4 – 6]. It can be inferred from statistical data [4 – 7] that time to rupture in bends subjected to internal pressure can be up to three times shorter than in straight portions of a pipeline. It is seen therefore that a sound assessment of strain magnitudes and their effect on structural material properties is of great importance to a designer of piping systems and especially – power pipelines [3 – 8].

The author believes that this analysis would have gained a lot from being confronted by a richer collection of experimental data. Unfortunately, he could not find the data other than for a particular bending angle of 180° . It is to be also noted that due to a wide range of outside diameters (4 – 600 mm) and wall thickness (0.2 – 50 mm), a single model is hardly capable of covering all combinations of pipe size and bending process parameters. Selection of a particular bending technique is influenced by various factors: type of material and pipe dimensions, bending radius and bending angle, dimensional accuracy required, size of production lots, type of intended pipeline application, etc.

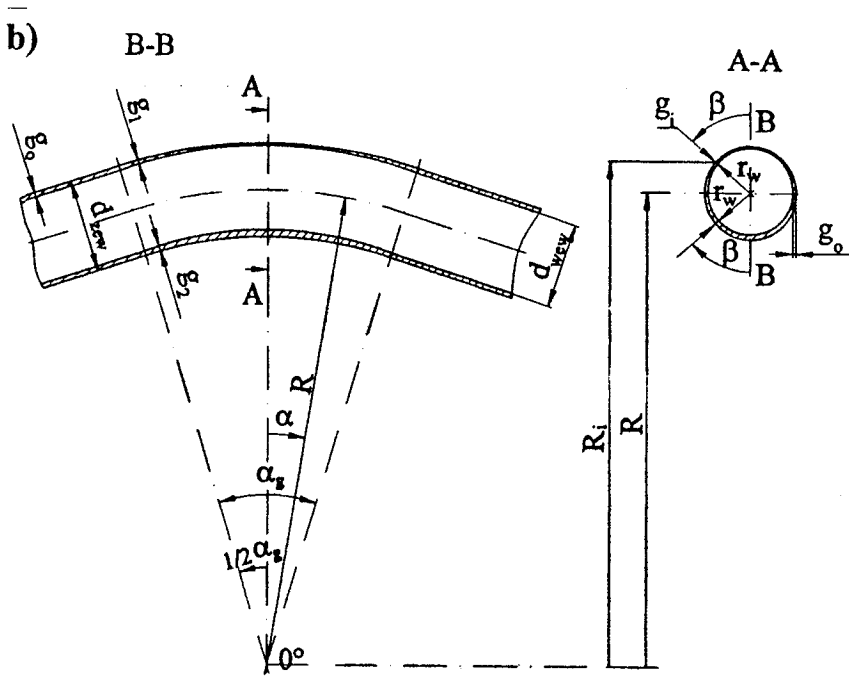


FIG. 1. a, b. Geometrical quantities in the pipe bending description.

3. BASIC RELATIONSHIPS

The condition of constant volume may be written as

$$(3.1) \quad R_i \cdot r_i \cdot g_i = R \cdot r_{out} \cdot g_0,$$

where

$$(3.2) \quad R_i = R_i(R, r_{in}, g_i, \alpha, \beta, k),$$

is the larger running bending radius whose precisely defined form is to be used in determining longitudinal strains, and

$$r_i = r_{in} + g_i, \quad r_{out} = \frac{d_{out}}{2}, \quad r_{in} = \frac{d_{in}}{2}, \quad r_{in} = r_{out} - g_0,$$

(subscript $i = 1$ and (+) sign refer to elongated fibres while $i = 2$ and (-) sign refer to compressed fibres).

It is reasonable to assume from the geometry of pipe bending that for the larger running radius R_i which is determined both within the zone of bending, and at the plane of bending the corresponding component measures may be given by

$$(3.3) \quad z_1 = (r_{\text{in}} + g_i) \cdot \cos \beta \left(\cos k\alpha - \cos k \frac{\alpha_g}{2} \right),$$

$$z_2 = (r_{\text{in}} + g_i) \cdot \beta \left(\sin k \frac{\alpha_g}{2} - \sin k\alpha \right),$$

i.e. z_1 and z_2 are vertical and horizontal measures, respectively.

A thorough analysis of the problem and comparison of the model data with experimental ones presented in [1, 2] led the author to use a formula for z_1 for the bending angle equal to 180° in the form put forward in the same source, namely

$$(3.4) \quad R_i = R \pm (r_{\text{in}} + g_i) \cdot \cos \beta \left(\cos k\alpha - \cos k \frac{\alpha_g}{2} \right).$$

The relationship is a very good approximation of the experimental data from [1, 2], especially for elongated fibres, as can be seen in the plots. It can be easily demonstrated that the two definitions in (2.2) become equivalent for $\alpha = \alpha_g/2$ and for ($k\alpha = 0^\circ$ and $k\alpha_g = 180^\circ$). When $k\alpha = 0^\circ$, then $\alpha = 0^\circ$, since $k \neq 0$.

$$(3.5) \quad \ln \frac{R_i}{R} + \ln \frac{r_i}{r_z} + \ln \frac{g_i}{g_0} = 0,$$

where

$$\varphi_1 = \ln \frac{R_i}{R}, \quad \varphi_2 = \ln \frac{r_i}{r_{\text{out}}}, \quad \varphi_3 = \ln \frac{g_i}{g_0}.$$

Hence, the condition of incompressibility is fulfilled:

$$(3.6) \quad \varphi_1 + \varphi_2 + \varphi_3 = 0.$$

Substitution of (2.3) into (2.4)₂₋₄ yields the following formulas:

$$(3.7) \quad \varphi_1 = \ln \frac{R \pm (r_{\text{in}} + g_i) \cdot \cos \beta \left(\cos k\alpha - \cos k \frac{\alpha_g}{2} \right)}{R},$$

$$\varphi_2 = \ln \frac{r_{\text{in}} + g_i}{r_{\text{out}}},$$

$$\varphi_3 = \ln \frac{g_i}{g_0}.$$

Intensity of strain has the following form [14 - 16]:

$$(3.8) \quad \varphi_i = \sqrt{\frac{2}{3} \left(\varphi_1^2 + \varphi_2^2 + \varphi_3^2 \right)}.$$

Inserting Eqs (3.6) into (3.5) and performing suitable transformations we arrive at the following algebraic equation of the third order with respect to the running thickness of a bend across the bending zone:

$$(3.9) \quad a \cdot g_i^3 + b \cdot g_i^2 + c \cdot g_i + d = 0,$$

where

$$a = \pm \left(\cos k\alpha - \cos k \frac{\alpha_g}{2} \right) \cdot \cos \beta,$$

$$b = \left[R \pm 2r_{in} \cdot \left(\cos k\alpha - \cos k \frac{\alpha_g}{2} \right) \cdot \cos \beta \right],$$

$$c = \left[R \pm r_{in} \left(\cos k\alpha - \cos k \frac{\alpha_g}{2} \right) \cdot \cos \beta \right] \cdot r_{in},$$

$$d = -R \cdot r_{out} g_0.$$

The equation is satisfied by a single real root that is a sought-for solution and two complex roots.

As can be seen, the running thickness g_i of a bend within the bending zone depends on: bending radius R , outside and inside pipe radii (r_{out} and r_{in}), initial thickness g_0 , bending angle α_g , angles α and β determining location of a point within the bending zone for fibres in tension and compression, respectively, and coefficient k of the range of bending within the bending zone.

The solution to the equation, the corresponding strain and intensity components were obtained using a computer program. The results are shown as plots juxtaposed with those representing test data after [2].

Solving a similar equation involving the second measure (3.2) resulted in faster changes of g_1 and larger values of measures φ_1 , φ_2 , φ_3 and φ_i within the bending zone. As was observed earlier, for $\alpha = \alpha_g/2$ and ($k\alpha = 0^\circ$; $k\alpha_g = 180^\circ$) the two representations become equivalent and the results are equal.

The second measure (3.2) should for processes involving larger changes in pipe wall thickness and higher values of strain and strain intensity components. It is to be noted that thickness and strain distributions resulting from adopting that measure for $k = 1$ were of doubtful value.

Throughout the whole plateau zone formulas (3.6) and (3.8) should be used with ($\cos k\alpha = 1$ and $\cos \alpha_g/2 = 0$), while the second measure (3.2) – with ($\sin k\alpha = 0$ and $\sin \alpha_g/2 = 1$). It should be added that Eq. (3.8) enables an inverse problem to be solved, i.e. a critical bending angle value α_{gcr} may be determined that corresponds to a critical wall thickness value at the wall apex

($\alpha = \beta = 0^\circ$). For the elongated fibres this will be obviously the lowest allowable thickness g_{1all} . The corresponding relationships then hold:

$$(3.10) \quad \varphi_{all} = \ln \frac{R + (r_{in} + g_{1all}) \cdot \left(1 - \cos k \frac{\alpha_{gcr}}{2}\right)}{R},$$

$$\varphi_2 = \ln \frac{r_{in} + g_{1all}}{r_{out}}, \quad \varphi_3 = \ln \frac{g_{1all}}{g_0},$$

and

$$(3.11) \quad a \cdot g_{1all}^3 + b \cdot g_{1all}^2 + c \cdot g_{1all} + d = 0,$$

where

$$a = \left(1 - \cos k \frac{\alpha_{gcr}}{2}\right),$$

$$b = \left[R + 2r_{in} \left(1 - \cos k \frac{\alpha_{gcr}}{2}\right)\right],$$

$$c = \left[R + r_{in} \cdot \left(1 - \cos k \frac{\alpha_{gcr}}{2}\right)\right] \cdot r_{in},$$

$$d = -R \cdot r_{out} g_0.$$

Hence

$$(3.12) \quad \cos \left(k \frac{\alpha_{gcr}}{2}\right) = 1 - R \cdot \frac{r_{out} \cdot g_0 - g_{1all}^2 - r_{in} \cdot g_{1all}}{g_{1all}^3 + 2 \cdot r_{in} \cdot g_{1all}^2 + r_{in}^2 \cdot g_{1all}}.$$

Proceeding in a similar way one determine a critical bending angle value α_{gcr} based on a value of φ_{iall} derived from the tensile test for a given material. For this purpose, formulas (3.7) and (3.9) or the plot φ_i from Fig. 5 are used for an assumed coefficient k value. Other parameters of the bending operation could be obtained from suitable nomograms (not available yet).

4. INITIAL AND BOUNDARY CONDITIONS

The relationship derived in Sec. 2 fulfil the following initial and boundary conditions:

a) when $\alpha = \frac{\alpha_g}{2} = 0$ - bending process begins (isn't bending)

b) $\alpha = \frac{\alpha_g}{2} \neq 0$ - beginning and end of the bending zone,

c) $\beta = 90^\circ$ - location of the neutral surface within the bending zone;

it follows then

$$(4.1) \quad R_i = R, \quad r_i = r_{\text{out}}, \quad g_i = g_0$$

and

$$\varphi_1 = \varphi_2 = \varphi_3 = 0, \quad \varphi_i = 0;$$

d) $k\alpha = \beta = 0^\circ$ – apex point of the bending zone;
if, additionally, $k\alpha_g \in (0^\circ; 180^\circ)$, then
to

$$(4.2) \quad R_i = R \pm (r_{\text{in}} + g_i) \cdot \left(1 - \cos\left(k \frac{\alpha_g}{2}\right)\right),$$

$$r_i = r_{\text{in}} + g_i;$$

e) if $k\alpha = \beta = 0^\circ$ and $k\alpha_g = 180^\circ$, then the quantities R_i , r_i and g_i reach their extremes (maximum or minimum values). At the same time this is the condition for the onset of the plateau zone at this point.

For the elongated fibres we get the following expressions:

$$(4.3) \quad g_1 = g_{\text{min}},$$

$$R_1 = R + (r_{\text{in}} + g_{\text{min}}),$$

$$r_1 = r_{\text{in}} + g_{\text{min}},$$

and for the compressed ones

$$(4.4) \quad g_2 = g_{\text{max}},$$

$$R_2 = R - (r_{\text{in}} + g_{\text{max}}),$$

$$r_2 = r_{\text{in}} + g_{\text{max}}.$$

The coefficients a, b, c present in Eq. (3.7) will assume in this case the following form:

$$(4.5) \quad a = 1,$$

$$b = (R \pm 2 \cdot r_{\text{in}}),$$

$$c = (R \pm r_{\text{in}}) \cdot r_{\text{in}},$$

while the coefficient $d = -R \cdot r_z \cdot g_0$ will remain the same.

Principal components of the logarithmic strains and strain intensity also reach their extremes but these are different for each type of fibres.

EXAMPLE

The plots yield the following values:

elongated fibres	compressed fibres
$g_{\min} \cong 3.684$	$g_{\max} \cong 5.99$
$r_1 = 21.434$	$r_2 = 23.746$
$R_1 = 101.434$	$R_2 = 56.254$
$\varphi_1 = 0.2553$	$\varphi_2 = 0.3748$

The above data may serve as a basis for determining the ovalization index accounting for the wall thickness being different when measured across the areas in tension and compression. For the sake of clarity we take the middle point of a bend or, in other words, the apex point of the bending zone for $k = 1$.

According to [1]

$$(4.6) \quad e = \frac{d_1 - d_2}{d_2} \cdot 100\%,$$

where

$$\begin{aligned} d_1 &= 2r_{\text{in}} + g_{\min} + g_{\max}, \\ d_1 &= 2 \cdot 17.75 + 3.684 + 5.996, \\ d_1 &= 45.18 \end{aligned}$$

and $d_2 = d_{\text{out}}$ to comply with assumptions listed in Sec. 1.

Hence $e \cong 1.53\%$.

According to [5]

$$(4.7) \quad A = \frac{2 \cdot (d_1 - d_2)}{d_1 + d_2} \cdot 100\%$$

hence $A \cong 1.52\%$.

5. ANALYSIS OF THE RESULTS

Figure 2 presents computational results for the wall thickness g_1 at the elongated fibre area *vs* bending angle at a point with angle coordinates $k\alpha = \beta = 0^\circ$ (apex point of the bending zone) for pipe OD 44.5×4.5 , $R = 80$ mm ($R = 1.8 \times d_{\text{out}}$) made of St 35.8 steel according to DIN 17175 [2].

The forthcoming discussion will be concerned primarily with the behaviour of elongated fibres since they conform to the theory particularly well. The compressed fibres will be discussed only in a short commentary due to severe shortcoming of the model in those areas.

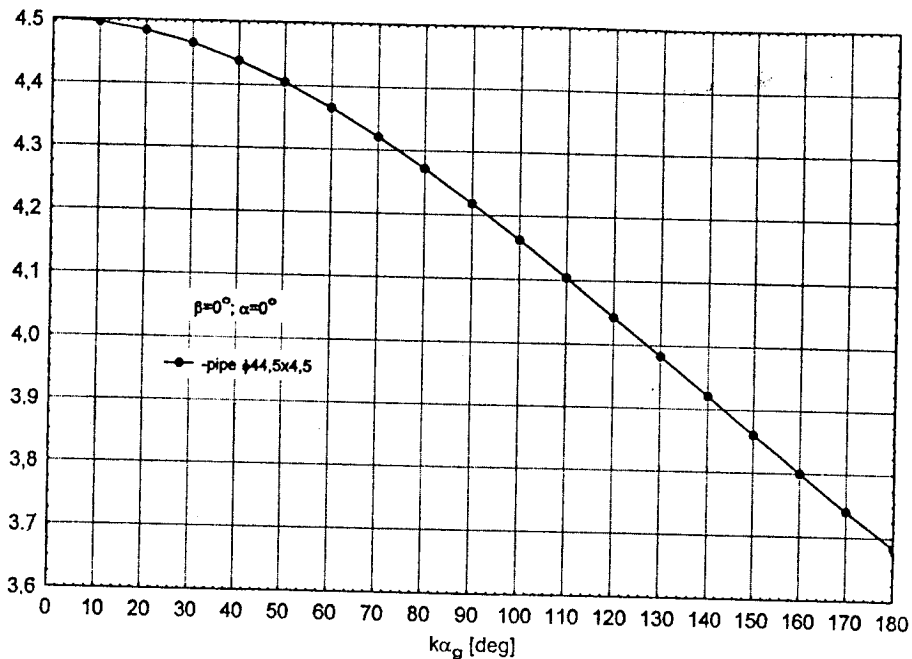


FIG. 2. Variation of the wall thickness at the apex point of the elongated area.

Figure 3 gives a comparison of results obtained from equations derived in Sec. 2 of this paper with those obtained from tests presented in [2]. The bending angle was $\alpha_0 = 180^\circ$ as measured at the principal plane of bending, i.e. for $\beta = 0^\circ$. As can be seen from the plot, the $\varphi_1, \varphi_2, \varphi_3$ values for the apex point of the bending zone ($\alpha = \beta = 0^\circ$) and within the elongated fibre area are in very good agreement with the experimental data. They do not coincide so well for the whole angle range ξ - but the discrepancy can be readily explained: ideal conditions of bending assumed in the model differ from the actual ones which involve friction, a projecting mandrel and the limited value of $k = 1$. It can be noted that for $k = 3$ the calculated and experimental values agree fairly well, especially for the left-hand half of the plots in Fig. 3, both the bending zone and plateau zone. For the right-hand side of Fig. 3, the bending zone may be adequately represented by the second measure (3.2) or a combination of the two-their arithmetic or geometric mean. The above statements were confirmed by the author when his calculated data were compared with experimental ones quoted in [1, 2]. The other data in [2] obtained in tests using either a not-projecting mandrel or no mandrel at all conform well with the author's theory if one assumes $k = 2.5$.

For bending with and without a mandrel, the calculated results were also in fairly good qualitative and quantitative agreement with test data contained in [1] if one assumed $k = 1$ for the no-mandrel case and $k = 2$ for the other.

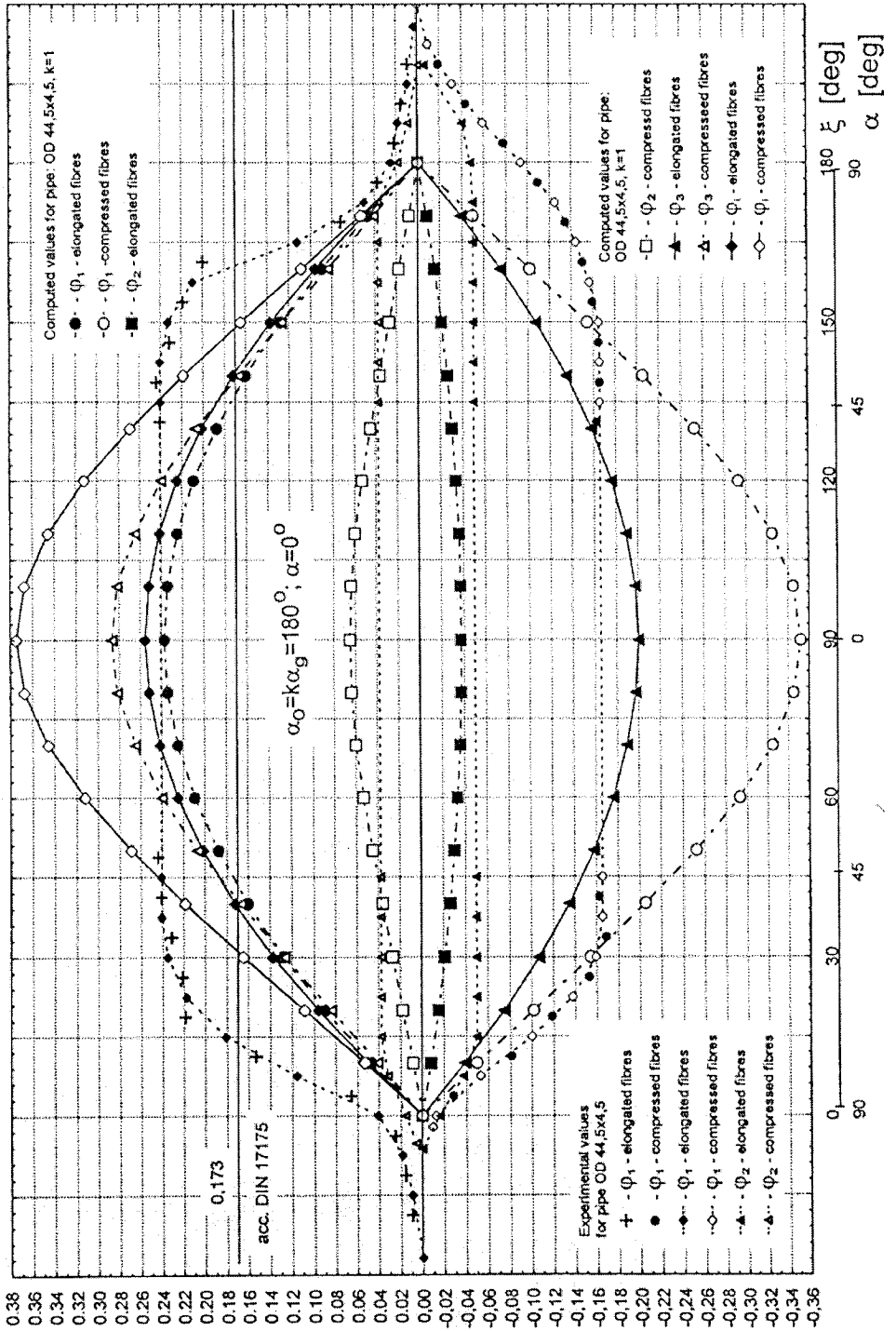


FIG. 3. Plots of strains at the bending plane: after [2] the calculated ones.

The bending zone-plateau zone ratio deserves a short commentary. If $k = 1$, then the whole zone defined by the range $[0^\circ; 180^\circ]$ is the bending zone without the plateau portion. When k tends to infinity, then the bending zone extent tends to zero and the whole bend area is occupied by the plateau zone. The running wall thickness g_i is then constant and at the bend ends a sharp change in thickness occur, so to that $g_i \neq g_0$ ($g_i < g_0$) for elongated fibres and $g_i > g_0$ for compressed ones). The strains φ_i , φ_1 and thickness g_i depend solely upon angle β rather than on angles α and α_g . The obvious conclusion is that for each value of k belonging to the set $k \in [0^\circ; \infty)$ we have $\alpha_0 \geq \alpha_g$.

It follows from the presented bending operation model that the maximum angular range of bending portion is equal to 180° while the bend angle range is, at least in theory, unlimited. The difference $(\alpha_0 - \alpha_g)$ - between the bending angle and bend angle gives the plateau zone range.

It can be generally stated that coefficient k becomes larger, firstly, with decreasing bending radius R , secondly, if a more projecting and stiffer mandrel is used and, thirdly, if thick-walled tubes fabricated of less ductile material are involved. A real value of k is also to some degree affected by a particular measurement method used and its accuracy.

It must be emphasized that for compressed fibres the model fails to predict true values of strains. The error may exceed then 100%, so the model was found to be applicable only to the elongated fibres of bent pipes.

Figure 4 is a transformed representation of data from Fig. 3, the transformation being from the principal plane of bending ($\beta = 0^\circ$) to the principal plane perpendicular to it ($\alpha = 0^\circ$). The data from Fig. 4 were compared with experimental data listed in [2, 6]. As a before, very good agreement was found for elongated fibres, the opposite being true for compressed fibres. This failure can be attributed to the fact that incompressible continuous medium is a very good approximation only for fibres in tension, both in thin- and thick-walled tubes. The compressed fibres in pipe bending behave differently. In bending with a mandrel, changes in wall thickness are small (a few percent, as demonstrated in [1]) and it can be safely assumed that in thin-walled pipes $g_2 \cong g_0$ in compressed areas [1]. Another phenomenon that is beyond the scope of the model is local buckling that is especially well pronounced in bending of thin-walled pipes. In order to arrive at a realistic picture of the pipe's behaviour, one has to remember that the neutral surface changes its position in a varying fashion depending on a particular technique used [11 - 14]. The present model assumes this position to be fixed and uniquely determined by bending radius R . It seems that in hot free bending of thick-walled tubes without a mandrel the model will offer an adequate picture of deformations. The assumed pattern of deformation occurring in the elongated fibre area was investigated at length elsewhere [15, 17 - 20]. The model of a thin

shell under plane stress worked out there proved to be very successful in fitting to test data. Those investigations served as guidance to the present author.

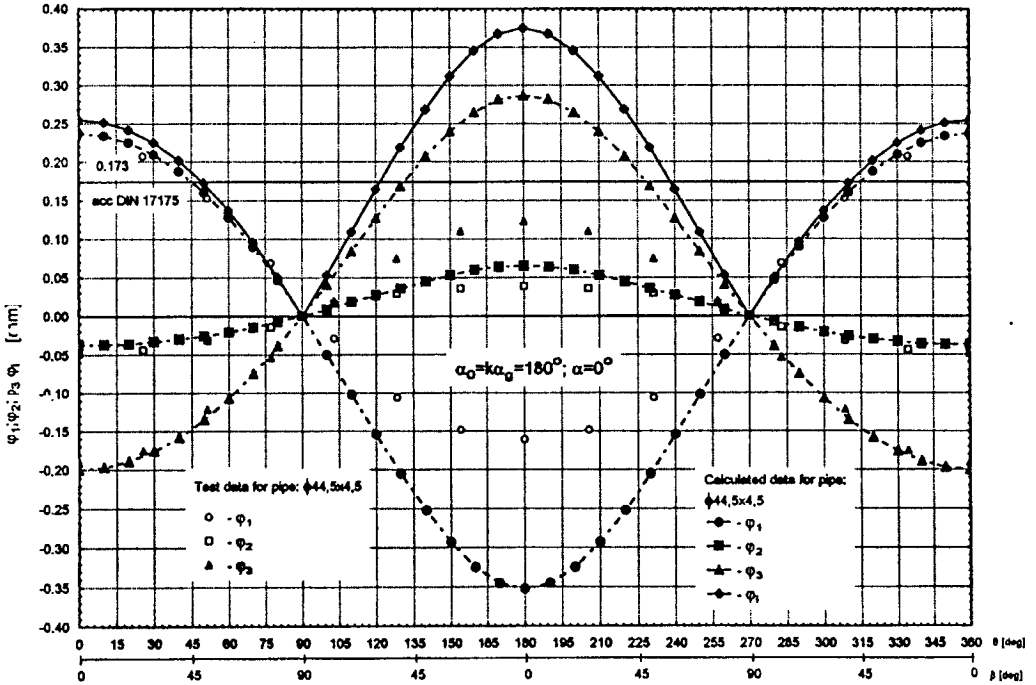


FIG. 4. Strains at planes perpendicular to the bending plane: after [2] the calculated ones.

Figure 5 present components of the logarithmic principal strains $\varphi_1, \varphi_2, \varphi_3$ and the equivalent strain φ_i as functions of bending angle $k\alpha_{gcr}$ for the apex point ($\alpha = \beta = 0^\circ$). By taking an ordinate equal to a permissible value of deformation determined for example in a uni-axial tensile test, we can find an allowable value of bending angle that must not be exceeded in order to keep deformation below a stipulated level [e.g. A_r (uniform) per cent elongation or A_5 -elongation]. Let us have a practical example. From [2] we have $\phi_1 = 0.173$ for St 35.8 acc. DIN17175 and the corresponding bending angle given by the plot is $k\alpha_g \cong 145^\circ$. It means that on exceeding this value, the outside stretched layers of a pipe (see Fig. 4, $0^\circ \leq \beta \leq 45^\circ$) will undergo deformation exceeding the uniform per cent elongation value. Plastic deformation at this stage gets unstable and necking occurs [6]. The wall thickness value g_1 at the bend apex point corresponding to $k\alpha_g \cong 145^\circ$ can be found from the plot in Fig. 2 to be equal to 3.9 mm.

Figure 6 shows variation of the wall thickness g_1 in the elongated fibre area at the principal plane of bending ($\beta = 0^\circ$) and the principal plane perpendicular to it ($\alpha = 0^\circ$), for bend angle $\alpha_0 = 180^\circ$ and bending angle $k\alpha_g = 180^\circ$. As can

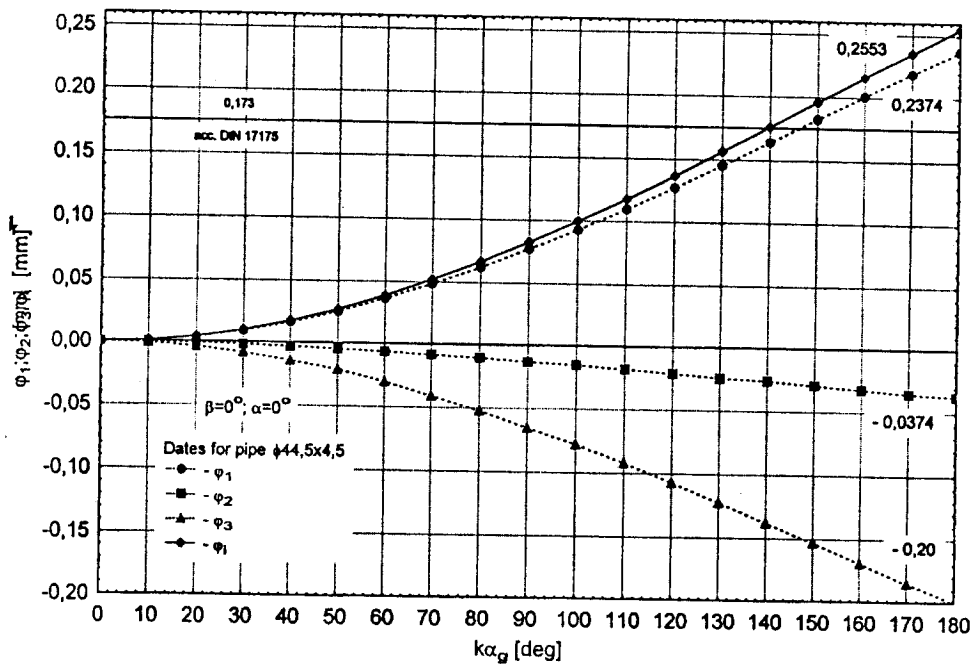


FIG. 5. Strain and strain intensity components as functions of bending angle.

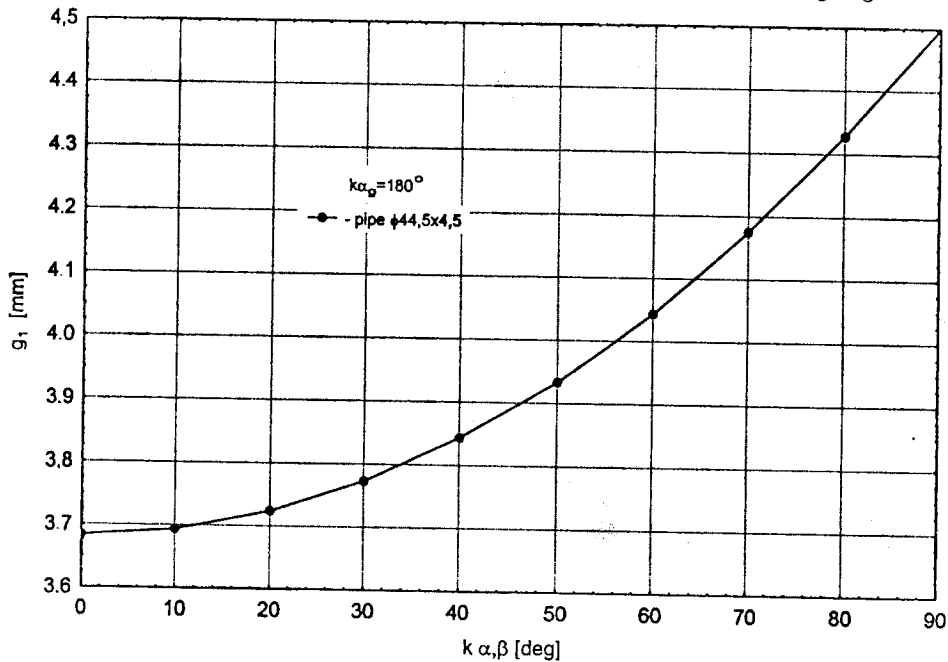


FIG. 6. Variation of wall thickness at the principal plane of bending and at planes perpendicular to it.

be seen, the two curves coincide which is a direct consequence of formulas (3.3), (3.6)₁ and (3.8). For other bending angles ($k\alpha_g \neq 180^\circ$) the plots will be separated.

6. FINAL REMARKS AND CONCLUSIONS

a. The calculated results prove that the proposed relationships are an adequate representation of the bending process for stretched layers of thin-walled pipes ($s < 0.2$) and for $\alpha_0 = k\alpha_g = 180^\circ$. The model fails to predict true values for the compressed fibres since it does not account for flattening of cross-section and buckling effects.

b. The inadequacy of the model in the compressed area will become less severe in hot bending of thick-walled pipes since the adverse effects of local buckling will then tend to diminish.

c. A refined form of the bending operation such as: bend angle α_0 or bending angle α_g , allowable minimum wall thickness g_{1all} . The last value sets a limit that must not be exceeded if local buckling or rupture are to be avoided.

d. Application of the second measure (3.2) for radius R_i will result in a thinner wall and larger deformation within the bending zone, i.e. will call for a more conservative assessment of the bending angle α_{gr} .

e. It is possible to arrive at simpler forms of the relationships derived in Sec. 2 by neglecting higher-order effects. Such simplified formulas could be useful in everyday engineering practice.

f. The inverse problem deserves to be noted. It could be stated as follows: what is the initial wall thickness g_0 if a given tube is to be bent with a given radius R and a given bend angle α_0 to reach the minimum allowable wall thickness value at the apex point of the stretched area, not smaller than that specified by structural analysis calculations and the Code requirements? The relevant theory should also account for conditions set by the Polish national standard [23] that sets allowable minimum wall thickness and deformation values such that the allowable strain intensity φ_{iall} or φ_{1all} does not exceed a stipulated value of (uniform) per cent elongation for tube material.

g. It is possible to introduce in a formal way some averaged measures for determining strains within the bending zone such as arithmetic or quadratic means of the component measures z_1 and z_2 . Such averaged measures – as can be readily proved – are also equal to the component measures (3.2) at particular points of the process, i.e. for $\alpha = \alpha_g/2$ and ($k\alpha = 0^\circ$; $k\alpha_g = 180^\circ$). It must be stressed that measure of the above kind lack any physical sense but are likely to improve accuracy of the results.

h. The presented theory might be supplemented with nomograms for simple determination of admissible values of the deformation measures: α_{0cr} , α_{gcr} , φ_{1all} , φ_{1all} , g_{1all} .

ACKNOWLEDGEMENTS

The author would like to thank Professor E.S. DZIDOWSKI (Wrocław University of Technology) for fruitful discussions and Mr. M. WOLSKI (M.Sc.Eng.) for his help in performing calculations and making figures.

REFERENCES

1. J.W. KORZEMSKI, *Bending of thin-walled pipes* [in Polish], WNT, Warszawa 1971.
2. W.D. FRANZ, *Das Kalt - Biegen von Rohren*, Springer - Verlag, Berlin 1961.
3. F. SEYNA, J. GINALSKI, *Long-term safe exploitation of steam pipelines* [in Polish], Energetyka, 6, 1987.
4. F. SEINA, J. GINALSKI, *Evaluation of residual life in steam pipelines* [in Polish], Dozór Techniczny, 3, 1989.
5. J. DOBOSIEWICZ, K. WOJCZYK, *Life assessment in steam pipeline bends* [in Polish], Energetyka, 3, 1998.
6. E.S. DZIDOWSKI, Sz. STRAUCHOLD, *Effect of technological factors in pipe bending on damage characteristics and reliability of power pipelines* [in Polish], Zeszyty Naukowe Politechniki Opolskiej, Seria Elektryka, z. 46, Opole 1998.
7. R.H. KOZŁOWSKI, *Selected material problems of conventional power engineering* [in Polish], Energetyka, 9, 1997.
8. Z. ŚLÓDERBACH, T. SAWICKI, *Thermomechanical coupling effect in thick-walled spheres and tubes subjected to internal pressure* [in Polish], IFTR-Reports - PAN, 16, Warszawa 1983.
9. W. OLSZAK, P. PERZYNA, A. SAWCZUK, *Theory of plasticity* [in Polish], PWN, Warszawa 1985.
10. W. SZCZEPIŃSKI, *Theory of plastic working metals* [in Polish], PWN, Warszawa 1969.
11. R. HILL, *Mathematical theory of plasticity*, Oxford, at the Clarendon Press, 1950.
12. M. ŻYCZKOWSKI, *Complex loading in theory of plasticity* [in Polish], PWN, Warszawa 1973.
13. K.H. RUHL, *Die Tragfähigkeit metallischer Baukörper*, Ernst & Sohn, Berlin 1952.
14. W. KRZYŚ, M. ŻYCZKOWSKI, *Selected problems in elasticity and plasticity* [in Polish], WNT, Warszawa 1962.
15. Z. MARCINIAK, *Limit deformations in sheet metal forming* [in Polish], WNT, Warszawa 1971.
16. J. GRONOSTAJSKI, *Plastic working of metals* [in Polish], Skrypt Politechniki Wrocławskiej, Wrocław 1973.

17. Z. MARCINIAK, *Stability of thin shells under plastic conditions* [in Polish], Rozpr. Inżyn., 1968.
18. Z. MARCINIAK, *Loss of stability in metals* [in Polish], Mech. Teoret. i Stos., Warszawa 1966.
19. Z. MARCINIAK, *Mechanics of sheet metal pressing* [in Polish], WNT, Warszawa 1961.
20. Z. ŚLÓDERBACH, T. SAWICKI, *Evaluation of the spherical cup height as used in the hydraulic pressing test as viewed by certain stability loss conditions* [in Polish], IFTR-Reports – PAN, 4, Warszawa 1984.
21. Z. ŚLÓDERBACH, *Assessment of plastic deformation localization states* [in Polish], WNT, Warszawa 1993.
22. Polska Norma, PN-89/M-34163, PKNM i J, Warszawa 1989.

Received August 13, 1998; revised version October 29, 1998; new version January 20, 1999.
